Backside Calibration Chronopotentiometry: Using Current to Perform Ion Measurements by Zeroing the Transmembrane Ion Flux

ARTICLE *in* ANALYTICAL CHEMISTRY · OCTOBER 2008

Impact Factor: 5.64 · DOI: 10.1021/ac800774e · Source: PubMed

4 AUTHORS, INCLUDING:

Eric Bakker
University of Geneva
291 PUBLICATIONS **13,793** CITATIONS

Published in final edited form as:
Anal Chem. 2008 October 1; 80(19): 7516–7523. doi:10.1021/ac800774e.

Backside Calibration Chronopotentiometry: Using Current to Perform Ion Measurements by Zeroing the Transmembrane Ion Flux

Yida Xu[1], **Wittaya Ngeontae**[1,2], **Ernö Pretsch**[3], and **Eric Bakker**[1,4]

[1]*Department of Chemistry, Purdue University, West Lafayette, Indiana 47907* [2]*Environmental Analysis Research Unit and Supramolecular Chemistry Research Unit, Department of Chemistry, Faculty of Science, Chulalongkorn University, Bangkok, Thailand, 10330* [3]*Institute of Biogeochemistry and Pollutant Dynamics, ETH Zurich, CH-8092 Zurich, Switzerland* [4]*Nanochemistry Research Institute, Department of Applied Chemistry, Curtin University of Technology, GPO U1987, Perth, WA 9845, Australia.*

Abstract

A recent new direction in ion-selective electrode (ISE) research utilizes a stir effect to indicate the disappearance of an ion concentration gradient across a thin ion-selective membrane. This zeroing experiment allows one to evaluate the equilibrium relationship between front and backside solutions contacting the membrane by varying the backside solution composition. This method is attractive since the absolute potential during the measurement is not required, thus avoiding standard recalibrations from the sample solution and a careful control of the reference electrode potential. We report here on a new concept to alleviate the need to continuously vary the composition of the backside solution. Instead, transmembrane ion fluxes are counterbalanced at an imposed critical current. A theoretical model illustrates the relationship between the magnitude of this critical current and the concentration of analyte and countertransporting ions, and is found to correspond well with experimental results. The approach is demonstrated with lead(II)-selective membranes and protons as dominating interference ions, and the concentration of Pb^{2+} was successfully measured in tap water samples. The principle was further evaluated with calcium-selective membranes and magnesium as counterdiffusing species, with good results. Advantages and limitations arising from the kinetic nature of the perturbation technique are discussed.

Conventional ion-selective electrode measurements are dependent on the emf difference between the indicator and a reference electrode, and the phase boundary potential between the sample solution and the ion-selective membrane is regarded as the determining factor if other potential contributions can be minimized. Thus, the stability of the potential at the inner and outer reference electrode is of critical importance with ISE measurements, and a strict temperature control and recalibration of the electrodes are always necessary in real world sample analyses. This hampers the application of this technology to remote sensing or in-vivo applications where strict recalibration protocols are not achievable.[1, 2]

Recently, a new direction in ISE research, coined backside calibration potentiometry, was introduced to help solve this problem.[3] In this new technique, the exact value of the cell potential is no longer important. Instead, the method utilizes thin ion-selective membranes where a mismatch of the front and backside solution composition results in a spontaneous ion

[2] Present address: Department of Chemistry, Faculty of Science, Khon Kaen University, Khon Kaen, 40002 Thailand.

flux across the membrane.[4] The existence of this flux is evaluated potentiometrically by changing the stirring or flow rate of the contacting solutions. Disappearance of the stir effect upon changing the ionic composition at the back side indicates that the front and back side solutions are chemically matched in terms of their ion-exchange equilibrium with the membrane phase. A relatively thin Celgard ISE membrane is used for the measurement,[5] which makes it possible to establish steady-state concentration gradients within a few minutes.[3, 4] The feasibility for real world sample analysis was demonstrated by measuring free lead ion concentration in tap and river water samples.[3]

The sensitivity and working range of backside calibration potentiometry was subsequently explored.[6] Unlike classical potentiometry, the sensitivity in backside calibration potentiometry is dependent on the magnitude of potential jump upon the change of stirring rate, and it is related to the primary ion concentration difference between the two sides of the membrane. A logarithmic concentration ratio of about 0.05 is still detectable under optimized conditions. A bell shaped response curve is observed for the working range that spans about 3 orders of magnitude of primary ion concentration and that can be shifted to some extent.[6] It must be noted that the disappearance of the stirring effect does not necessarily indicate an equal concentration of primary ions on the two sides of the membrane, since the concentration of counterdiffusion ion (the interference) is also important.[3]

Here, a novel approach to the concept of backside calibration potentiometry is explored for the first time. Instead of a continuous alteration of the backside concentration, an external current at the sub-nanoampere scale is applied across the membrane to counter the direction of the spontaneous ion flux of primary ions. The amount of current needed is determined by the disappearance of the stirring effect, in analogy to the method described above. Note that researchers utilized an applied current to lower the detection limit of conventional ISEs,[7-11] since undesired zero-current trans-membrane ion fluxes are the key reasons that ISEs can often not reach the thermodynamically predicted detection limits.[12-14] Unfortunately, however, this is difficult to do effectively for unknown samples and for systems where steady-state concentration gradients are established in a matter of hours. In this work, some of these limitations are circumvented by the use of thin membranes where steady-state is reached in minutes, and by using the potential as an indicator for the disappearance of a stir effect. For this reason, the absolute potential value is not important.

Theory

We consider a one-dimensional diffusion problem at steady state, owing to the rapid diffusion across the ion-selective membrane. The membrane potential of interest is a function of the phase boundary concentrations c_{if} and c_{ib} of the primary ion, i, at the front and back side of the membrane, respectively. If ion fluxes are relevant, these local concentrations will deviate from their bulk values, c_{ifb} and c_{ibb}, respectively. Since the expected influence of concentration changes in the membrane phase on the membrane potential will be negligible, one may formulate the membrane potential E_M in simplified form as follows, neglecting membrane diffusion potentials and assuming activity coefficients of unity:[15]

$$E_M = \frac{RT}{z_i F} \ln \frac{c_{if}}{c_{ib}} \quad (1)$$

where z_i is the valency of the ion i, and R and T have their established meanings.

The net flux induced at the front side of the membrane can be expressed as the sum of the individual ion fluxes of the counterdiffusing species:

$$J_c = z_i \rho_{aq} \left(c_{if} - c_{ifb} \right) + z_j \rho_{aq} \left(c_{if} - c_{jfb} \right) \quad (2)$$

Where J_c is the net ion flux across the membrane and c_{jf} and c_{jfb} are the concentrations of the exchanging ion (interference) in the phase boundary and bulk solution at the front side of the membrane. This treatment assumes that the only mode of transport across the membrane is by diffusion through ion-exchange with *j*. This may be valid at low concentrations of primary ion where coextraction processes are insignificant. Note that migration effects are not considered here because of the extremely small applied current densities. Recent work using ca. 100-fold larger current densities showed indeed that migration effects are no longer negligible.[16] The simplifying parameter ρ_{aq} is the ratio of the diffusion coefficient and diffusion layer thickness in the indicated phase, $\rho_{aq} = D_{aq} / \delta_{aq}$. For the membrane phase will write $\rho_m = D_m / \delta_m$, where δ_m is the membrane thickness. For simplicity, it is assumed that ρ_{aq} and ρ_m are equal for both ions under consideration. The net flux can be expressed in terms of an applied current, I_c, and one may write:

$$J_c = \frac{I_c}{FA_r} \tag{3}$$

Where A_r is the exposed membrane area. J_c in eq 2 is replaced by the right hand side of eq 3 to give:

$$\frac{I_c}{FA_r} = z_i \rho_{aq} \left(c_{if} - c_{ifb} \right) + z_j \rho_{aq} \left(c_{jf} - c_{jfb} \right) \tag{4}$$

Under symmetrical geometrical and stirring conditions, ρ_{aq} is the same for the back side of the membrane, and one may write in complete analogy:

$$\frac{I_c}{FA_r} = z_i \rho_{aq} \left(c_{ibb} - c_{ib} \right) + z_j \rho_{aq} \left(c_{jbb} - c_{jb} \right) \tag{5}$$

One may assume that each ion in the membrane is complexed by the ionophore L with a fixed stoichiometry n_i and n_j to form the species IL_{ni} and JL_{nj} for the ions *i* and *j*, respectively. The situation is subsequently formulated for the membrane phase in similar terms as above:

$$\frac{I_c}{FA_r} = z_i \rho_m \left([IL_{ni}]_b - [IL_{ni}]_f \right) + z_j \rho_m \left(\left[JL_{nj} \right]_b - \left[JL_{nj} \right]_f \right) \tag{6}$$

where square brackets denote the concentrations of the indicated species and the subscripts *f* and *b* relate to the front and back side of the membrane. A net gradient of ion-ionophore complex must result in a gradient of lipophilic ion-exchanger, R^-, for electroneutrality reasons.[17, 18] For the front side of the membrane, the ion-exchanger concentration, $R^-_{T,f}$, is expressed as:

$$R^-_{T,f} = z_i [IL_{ni}]_f + z_j \left[JL_{nj} \right]_f \tag{7}$$

And, in analogy, for the back side of the membrane, the ion-exchanger concentration, $R^-_{T,b}$, is written as:

$$R^-_{T,b} = 2R^-_T - R^-_{T,f} = z_i [IL_{ni}]_b + z_j \left[JL_{nj} \right]_b \tag{8}$$

where R^-_T is the average concentration of ion-exchanger in the membrane. Equations 7 and 8 are inserted into eq 6 to give the simplifed relationship:

$$\frac{I_c}{FA_r} = 2\rho_m \left(R^-_T - R^-_{T,f} \right) \tag{9}$$

The ion-exchanger concentration at the front side of the membrane is related to the phase boundary ion activities in the contacting sample solutions by ion-exchange equilibrium, which is conveniently expressed with established selectivity formalisms,[19] where K^{pot}_{ij} is the

selectivity coefficient. For a divalent ion *i* and a single type of monovalent ion *j* one may write:[20, 21]

$$\frac{c_{if}+\sqrt{c_{if}K_{ij}^{pot}c_{jfb}}}{c_{if}}=\frac{R_{T,f}^{-}}{2[IL_{ni}]_f} \tag{10}$$

If the same type of ions are present, one obtains for the back side in complete analogy:

$$\frac{c_{ib}+\sqrt{c_{ib}K_{ij}^{pot}c_{jbb}}}{c_{ib}}=\frac{2R_T^{-}-R_{T,f}^{-}}{2[IL_{ni}]_b} \tag{11}$$

It is here assumed that the exchanging ion, *j*, is present in excess relative to the concentration of the primary ion, and c_{jf} and c_{jb} in eqs 10 and 11 are approximated by their bulk solution concentrations, c_{jfb} and c_{jbb}. At steady state and under symmetrical stirring conditions, the concentration gradients at the front and back side of the membrane are related as follows:[4]

$$c_{ib}-c_{ibb}=c_{ifb}-c_{if} \tag{12}$$

The concentration gradients in the membrane and in the contacting front solution may be expressed as established:[22]

$$q=\frac{\rho_m}{\rho_{aq}}=\frac{c_{ifb}-c_{if}}{[IL_{ni}]_f-[IL_{ni}]_b} \tag{13}$$

Elimination of the four variables c_{ib}, $[IL_{ni}]_f$, $[IL_{ni}]_b$ *and* $R_{T,f}^{-}$ from eqs 9-13 gives the following implicit equation describing the dependence of c_{if} on experimentally available parameters:

$$\frac{4FA_r\rho_m\left(c_{if}-c_{ifb}\right)}{q}=\frac{\left(I_c-2FA_r\rho_mR_T^{-}\right)\sqrt{c_{if}}}{\sqrt{c_{if}}+c_{jfb}\sqrt{K_{ij}^{pot}}}+\frac{\left(I_c+2FA_r\rho_mR_T^{-}\right)\sqrt{c_{ibb}-c_{if}+c_{ifb}}}{\sqrt{c_{ibb}-c_{if}+c_{ifb}}+c_{jbb}\sqrt{K_{ij}^{pot}}} \tag{14}$$

This equation can be solved for c_{if} with appropriate software and inserted into eq 12 to yield c_{ib}, which is used with eq 1 to predict the membrane potential.

Note that kinetic parameters remain part of eq 14. The relationship between applied current and concentration changes will be reproducible if diffusion coefficients and diffusion layer thicknesses are experimentally repeatable as well.

Experimental

Reagents

Celgard 2500 polypropylene membranes were gracefully provided by Celgard Inc. (Charlotte, NC). The typical parameters are as following: porosity 55%, pore size 0.209 × 0.054 μm^2 and thickness 25 μm. 4-*tert*-butylcalix[4]-arene tetrakis(thioacetic acid dimethylamide) (lead ionophore IV), sodium tetrakis[3,5-bis(trifluoromethyl)phenyl]-borate (NaTFPB), tetradodecylammonium tetrakis(4-chlorophenyl) borate (ETH 500), bis(2-ethylhexyl) sebacate (DOS) and tetrahydrofuran (THF) were of Selectophore grade and purchased from Fluka. *N*,*N*-Dicyclohexyl-*N*′-phenyl-*N*′-3-(2-propenoyl)-oxyphenyl-3-oxapentanediamide (AU-1) was synthesized in our group.[23] Aqueous solutions were prepared with deionized water with a specific resistance of 18.2 MΩ·cm. High purity nitric acid and the aqueous lead nitrate standard solutions (0.1 M) were obtained from Fluka.

Membranes

For backside calibration measurements, the Pb^{2+}-selective Celgard-based membranes were prepared by soaking the membrane in a cocktail containing 0.65 mg (5 mmol·kg^{-1}, 0.46 wt %)

NaTFPB, 2.36 mg (16 mmol·kg^{-1},1.69 wt %) lead ionophore IV, 136.99 mg (97.9 wt %) DOS and 1 mL THF or 0.65 mg (5 mmol·kg^{-1}, 0.46 wt %) NaTFPB, 2.36 mg (16 mmol·kg^{-1},1.69 wt %) lead ionophore IV, 14.00 mg (10 wt %) ETH 500, 122.99 mg (97.9 wt %) DOS and 1 mL THF. After the membrane became transparent, it was first conditioned in 1 mM Pb$(NO_3)_2$ solution for 30 min, then washed with deionized (DI) water and conditioned in Pb$(NO_3)_2$ solution with the concentration equal to the lower concentration of Pb$(NO_3)_2$ solutions in the two chambers for another 30 min. After that, the membrane was again washed with DI water, dried with low lint absorbent tissue wipers and assembled into a Teflon cell with an exposed area of 0.79 cm^2. The Ca^{2+}-selective membranes were prepared in the same way, and the cocktail contained 0.65 mg (5 mmol·kg^{-1}, 0.46 wt %) NaTFPB, 1.46 mg (20 mmol·kg^{-1}, 1.46 wt %) Au-1 and 138.18 mg (98.5 wt %) DOS and 1 mL THF. The Ca^{2+}-selective membranes were conditioned in $Ca(NO_3)_2$ solutions instead of Pb$(NO_3)_2$ solutions. For low detection limit zero-current potentiometry measurements, the Pb^{2+}-selective PVC based membrane contained 0.68 mmol·kg^{-1} lead ionophore IV, 0.36 mmol·kg^{-1} NaTFPB, 11.46 mmol·kg^{-1} ETH 500, 36.55 wt % PVC, 62.04 wt % DOS and 0.15 mmol·kg^{-1} Pb$(NO_3)_2$. The membrane was solvent cast by dissolving all components except Pb$(NO_3)_2$ in 2.2 g THF, then 35.7 μL 1 mM Pb$(NO_3)_2$ solution (diluted from 0.1 M standard Pb$(NO_3)_2$ solution) was added, shaken to mix, and poured into a 2.8 cm i.d. glass ring fixed on a glass plate.

Electrochemical Characterization

Current-modulated backside calibration potentiometry measurements were conducted with a CH 910 bipotentiostat (CH Instruments InC., Austin, TX) at ambient temperature, using traditional 3-electrode set-up. During the measurements, the solutions in the symmetrical Teflon cell (20 mL cell volumes on both sides) were magnetically stirred or unstirred as indicated as with the non-current backside calibration potentiometry experiments reported previously.[3, 6] Two electrodes were Metrohm double junction Ag/AgCl reference electrodes with 1 M ammonium nitrate as bridge electrolyte, one used as working electrode with 1 M KCl as reference electrolyte in the backside chamber and the other used as reference electrode with 3 M KCl as reference electrolyte. A coiled platinum wire was used as counter electrode. Both counter electrode and reference electrode (with 3 M KCl) were positioned in the front side chamber. Zero-current potentials were measured with a 4-channel high impedance interface (World Precision Instruments, Sarasota, FL), a DAQ6015 data acquisition board and Labview 7.1 software (both from National Instruments, Austin, TX). The electrodes were conditioned in 1 mM $CaCl_2$, 0.1 mM HNO_3 and 1 nM Pb$(NO_3)_2$ for at least 24 h with an inner filling solution identical to the condition solution. Less than 0.2 mV potential change was considered as the indicator for the disappearance of the stirring effect. In general, usually 4 or 5 different currents needed to be applied to find the critical current, at up to 5 min each, giving a total analysis time of typically 20 to 30 min for each unknown sample concentration.

Calculations

All equations were solved with Mathematica (Version 5.2, Wolfram Research, Champain, IL). The kinetic parameters used in the calculations were as follows: For membranes without ETH 500, q = 1.57 (stirred) and 5.25 (unstirred) are from the reference[6] and ρ_m =2.2 × 10^{-5} dm·s^{-1} from the theoretical fit to the experimental data; For membranes with ETH 500, q = 0.57 (stirred) and 1.91 (unstirred) and ρ_m = 8 × 10^{-6} dm·s^{-1} are from the fit with the experimental data. The diffusion coefficients D_m used, 5.5 × 10^{-7} cm^2·s^{-1} and 2 × 10^{-7} cm^2·s^{-1} for membranes without and with ETH 500, respectively, are close to reported literature values.[24]

Results and Discussion

In current-less backside calibration potentiometry, the net ion flux across the membrane is always zero. The primary ion concentration gradient is equivalent to that of the counterdiffusing ion, but in the opposite direction. A concentration polarization of the (more dilute) primary ion will give rise to a stirring effect, where the observed potential changes as the stirring rate of the solution is altered. As the back side composition of the membrane is altered to achieve the disappearance of this stir effect, all transmembrane concentration gradients are expected to disappear and the three-phase system is at electrochemical equilibrium. In this work, a current is applied across the membrane to compensate the spontaneous ion flux, which eliminates the need for complicated fluidics at the back side of the membrane. The membrane is sufficiently thin and the concentration profiles in the system reach their steady-state values in a matter of minutes. This makes the experiment much more robust than earlier efforts on using currents to compensate fluxes to lower the detection limit of ion-selective electrodes containing comparatively thick membranes and slower diffusing components. [7-9, 11]

Figure 1 illustrates concentration profiles of a divalent primary ion and a counterdiffusion monovalent interference at three different applied currents. At steady state, the net flux from both ions will be equal to the flux induced by the applied current. The flux of primary ion is diminished at larger imposed currents, and as a consequence, the flux of interfering ions increases further. A critical current is reached when the primary ion flux becomes compensated, with a resulting disappearance of the concentration gradient. At this point, in contrast to currentless backside calibration potentiometry, the flux of the counterdiffusing ion does not disappear. The primary ion flux will change direction with a further increase of the current density, while the flux of originally counterdiffusing ion increases further, now in the same direction to that of the primary ions. This process is dependent on the selectivity coefficient of the membrane and the concentrations of ions involved. Since the primary ions are expected to be potential determining, the critical current is found at the point of zero stir effect: the influence of convective stirring on the observed potential disappears at this point.

Figure 2A explains more quantitatively the change in aqueous phase boundary lead ion concentrations at the front and back side of the membrane as a function of the applied current, with and without solution stirring, respectively. The bulk lead concentrations were chosen as $10^{-7.0}$ and $10^{-6.8}$ M in the front and back side for a most sensitive potential change with the parameters chosen here.[6] A kinetic parameter q of 1.57 and 5.25 was used for stirring and non-stirring conditions, respectively. According to Figure 2, all phase boundary lead ion concentration changes exhibit linear relationships with the applied current, and so does the expected magnitude of the potential jump upon stopping the sample stirring, see Fig. 2b. The phase boundary lead concentrations decrease at the font side and increase at the back side with increasing current, which is a result of the diminishing gradient of lead ions in direction of the sample (see also Figure 1). The magnitude of the observed slopes in Figure 2A is higher under non-stirring conditions than under stirring conditions, forming the basis for the measurement. The critical current that gives a zero potential change, shown with dotted lines, is used as the sensor signal.

Note, however, that the initial concentration gradients of lead ions under stirring and non-stirring conditions are different from each other. Intuitively, therefore, a different applied current would be needed to perfectly compensate each situation exhibiting a different q value. To illustrate the effect of q on the calculated critical current, the changes of front and back side concentrations with an applied current very close to the zero potential change are shown in Figs 3a and 3b. The currents needed to exactly compensate for the the primary ion flux while stirring the sample is indicated as I_s, while the compensating current for the unstirred sample is shown as I_u. Clearly, these two current values are not exactly the same and do not correspond

to the experimentally observed critical current, I_c, that gives a zero stir effect. At the critical current, therefore, primary ion fluxes are drastically reduced, but not perfectly compensated. The relationship between I_c, I_s and I_u is dependent on the kinetic parameter q. When the critical current I_c is reached, the phase boundary concentration of the primary ion will be equal for stirred and unstirred conditions, shown as the intersection of the solid lines in Fig. 3a and 3b. It does not, however, exactly correspond to the bulk concentration, see dotted horizontal lines. Note that the deviation from ideal behavior is relatively small (less than 1% in sample concentration), and therefore primarily of mechanistic interest. This is true for q values of less than 10, which covers most practical situations.

The observed critical current that shows zero stir effect is expected to change as a function of the sample composition. Figure 4 presents experimental data for the observed critical current as a function of the lead ion concentration at the front side of the membrane. In this experiment, the back side solution was fixed at $10^{-6.8}$ M Pb^{2+}, while 10^{-4} M H^+ served as the dominating interference at both sides of the membrane. The dashed line describes the symmetrical situation, in which case ion fluxes disappear at a critical current of zero. Note that an excellent correspondence between theory and experiment is observed. The slope of the calibration curve shown in Fig. 4 is non-linear, with increasing slope as the concentration is decreased. One would intuitively assume that plotting the data as a function of logarithmic activity linearizes the function, but strict linear behavior was not achieved. A key difference between this technique and the reported current-less backside calibration potentiometry is the influence of kinetic parameters on the calibration curve. Changes in membrane diffusion coefficients, for instance, are here expected to change the relationship between applied current and concentration gradients, altering the appearance of the calibration curve. In current-less backside calibration potentiometry, compensation of fluxes is performed by changing the composition at the back side only, and no such effect is expected.[3] For this reason, the behavior of the same membrane but with additional inert lipophilic electrolyte, ETH 500, was chosen for comparative purposes. It is known that addition of ETH 500 will decrease the diffusion coefficient in the membrane phase,[24] increase the number of available charge carriers and have some bearing on the observed selectivity coefficient. The resulting calibration curve is also shown in Figure 4, and a flattening is observed relative to the experiment without ETH 500. The theoretical curve was obtained with different q values 0.57 and 1.91 for stirred and unstirred solutions, respectively, using an unmodified concentration of ion-exchanger, R_T and a ρ_m value of 8×10^{-6} dm·s^{-1}. The selectivity coefficient was left unchanged for the theoretical curve. The proposed method trades the convenience of current control for a reduced level of robustness: membrane composition changes may result in a change of the observed calibration curve.

The effect of concentration of the counterdiffusion ion on the magnitude of the critical current was also examined. Here, the lead ion concentrations were fixed at $10^{-7.0}$ and $10^{-6.8}$ M at the front and back side, respectively, and the hydrogen ion was kept at the same level on both sides of the membrane. No ETH 500 was added to the membrane cocktail. Figure 5 shows that the critical current exhibited a linear relationship in the examined hydrogen ion concentration range. This may seem surprising at first glance, since the critical current is primarily used to compensate the flux of the primary ion, not the interfering one. Note, however, that the interfering ion co-dictates the flux of primary ion by counterdiffusion and ion-exchange processes. Changes in its concentration must inevitably alter the critical current. This is examined in more detail in Figure 6. The concentrations of lead ions were chosen as $10^{-7.0}$ and $10^{-6.8}$ M at the front and back side while the counterdiffusing ion concentration was 10^{-4} M and 10^{-3} M in Fig. 6a and 6b, respectively. The slope of the lead ion concentration change at the phase boundary is clearly dependent on the hydrogen ion level. Two effects on the lead ion concentration profile take place when the concentration of hydrogen ions is increased 10-fold from 10^{-4} M to 10^{-3} M. First, the initial concentration gradient of lead ions

($C_{ifb} - C_{if}$) in the absence of applied current increases about two-fold. Second, the slope of the lead ion phase boundary concentration change versus current increase decreases about 5-fold (see slopes for ΔC_{if} in Figure 6a and b). These two effects result in a ca. 10-fold higher current to fully compensate the lead ion concentration gradient.

The real world usefulness of this new technique was demonstrated by determining the lead ion concentration in local West Lafayette tap water. The recorded potential–time traces of the measurement are presented in Figure 7, where the solution reservoirs at the front and back side of the membrane were filled with 4×10^{-8} M $Pb(NO_3)_2$ and tap water (in both cases with a pH adjusted to 4.0 with HNO_3), respectively. The membrane used was the same as in Figure 4, without ETH 500 doped. When the current reaches about 150 pA, a potential change upon stopping of sample stirring is no longer observed. This indicates the disappearance of the primary ion flux in accordance to previous work.[3] Note that for this particular sample, the potential change observed upon stopping sample stirring was less pronounced than with laboratory samples, which may be improved by moving to a better controlled fluidic system and an automated evaluation of the potential drifts. Similarly, increasing the stirring rate of the conventional magnetic stirrer should give larger signals, but at a cost of increased potential noise. Further improvements are most likely with a wall jet or other type of flow system. From the calibration curve, the free Pb^{2+} concentration is calculated as $(2.55 \pm 0.68) \times 10^{-8}$ M (n =3 with standard deviation from 3 different samples). The tap water sample was also measured with zero-current potentiometry via classical standard addition[20] and the result was found as $(4.12 \pm 0.52) \times 10^{-8}$ M (n =3), and this value was used as a guide in choosing the lead ion concentration in the backside solution. While the two data sets are not in perfect agreement, the correspondence is quite good considering the simplifying assumptions in the theory. Note that the absolute potential is around 5-7 mV, which corresponds well to theoretical expectations according to the Nernst equation..

We also examined another system to evaluate the universality of the new method. Calcium and magnesium ions were selected as primary and interference ions, respectively, because it is a divalent-divalent ion system. The membrane was calcium-selective and used AU-1 as calcium ionophore without ETH 500. Fig. 8 presents the critical compensating current needed with the change of bulk calcium ion concentration in the front side of the membrane, and the intersection of the dotted line and X-axis indicates the calcium ion concentration at the back side. The chamber in the backside was filled with $10^{-6.8}$ M calcium nitrate and both sides contained 1 mM magnesium nitrate. A good correlation between theory and experimental results was found with $K^{pot}_{CaMg} = -8.8$,[22] $\rho_m = 3.4 \times 10^{-5}$ dm·s^{-1}, and q =1.57 and 5.25 for stirring and non-stirring conditions.

Conclusions

We explored here the use of sub-nanoampere scaled current to compensate the spontaneous zero-current ion flux in a new variation on the concept of backside calibration potentiometry. The primary model system was lead-selective and used protons as dominant interference. The magnitude of the critical current was found to depend on the concentration of primary ions and exhibited a linear relationship with the level of interference at a fixed primary ion concentration. The stirring rate does not influence the amount of critical current to a significant extent, which is one of the key reasons that this technique is applicable. The steady state can be usually achieved in just a few minutes. A theoretical model is established and it nicely agrees with the experimental results. The real world utility of this method is also examined with a real tap water sample and a calcium-magnesium system. The main advantage of this technique compared with current-less backside calibration potentiometry is that the solution in the backside does not need to be continuously changed to search for the appropriate solution composition to obtain a zero trans-membrane flux. Dialing in an appropriate current can be

accomplished much more easily. However, there are two main limitations in this technique. First, the reproducibility of the method may suffer if the system is subjected to long time exposure to higher current or stagnant solutions, which may induce compositional changes of the contacting solutions. This may be partly alleviated by the use of fluidics to repeatedly replace both solution chambers during the measurement. Similarly, the method appears to be best suited for systems where the sample composition is approximately known, in order to keep the required current densities relatively small. Second, compositional changes of the membrane over time will alter the kinetic characteristics of the system, which will have a bearing on the critical current needed to compensate the primary ion flux. In this respect, the convenience of using an applied current for zeroing the primary ion flux comes at the cost of achievable robustness.

Acknowledgments

This work was financially supported by the National Institutes of Health (EB002189 and GM07178). W.N. thanks The Development and Promotion of Science and Technology Talent Project (DPST) and The Institute for the Promotion of Teaching Science and Technology (IPST) for a scholarship.

Literature Cited

1. Meyerhoff ME. Trends Anal. Chem 1993;12:257–266.
2. Bakker E, Bhakthavatsalam V, Gemene KL. Talanta 2008;75:629–635. [PubMed: 18585124]
3. Malon A, Bakker E, Pretsch E. Anal. Chem 2007;79:632–638. [PubMed: 17222030]
4. Tompa K, Birbaum K, Malon A, Vigassy T, Bakker E, Pretsch E. Anal. Chem 2005;77:7801–7809. [PubMed: 16316191]
5. Ueberfeld J, Parthasarathy N, Zbinden H, Gisin N, Buffle J. Anal. Chem 2002;74:664–670. [PubMed: 11838692]
6. Ngeontae W, Xu Y, Xu C, Aeungmaitrepirom W, Tuntulani T, Pretsch E, Bakker E. Anal. Chem 2007;79:8705–8711. [PubMed: 17929899]
7. Pergel E, Gyurcsanyi RE, Toth K, Lindner E. Anal. Chem 2001;73:4249–4253. [PubMed: 11569816]
8. Lindner E, Gyurcsanyi RE, Buck RP. Electroanalysis 1999;11:695–702.
9. Michalska A. Electroanalysis 2005;17:400–407.
10. Morf WE, Badertscher M, Zwickl T, de Rooij NF, Pretsch E. J. Electroanal. Chem 2002;526:19–28.
11. Bedlechowicz I, Sokalski T, Lewenstam A, Maj-zurawska M. Sens. Actuators 2005;B108:836–839.
12. Sokalski T, Ceresa A, Zwickl T, Pretsch E. J. Am. Chem. Soc 1997;119:11347–11348.
13. Sutter J, Radu A, Peper S, Bakker E, Pretsch E. Anal. Chim. Acta 2004;523:53–59.
14. Bakker E, Pretsch E. Trends Anal. Chem 2005;24:199–207.
15. Bakker E, Buhlmann P, Pretsch E. Talanta 2004;63:3–20. [PubMed: 18969400]
16. Zook JM, Buck RP, Langmaier J, Lindner E. J. Phys. Chem. B 2008;112:2008–2015. [PubMed: 18217742]
17. Iglehart ML, Buck RP, Horvai G, Pungor E. Anal. Chem 1988;60:1018–1022. [PubMed: 3407944]
18. Moczar I, Gyurcsanyi RE, Huszthy P, Jagerszki G, Toth K, Lindner E. Electroanalysis 2006;18:1396–1407.
19. Bakker E, Meruva RK, Pretsch E, Meyerhoff ME. Anal. Chem 1994;66:3013–3020.
20. Ceresa A, Bakker E, Hattendorf B, Guenther D, Pretsch E. Anal. Chem 2001;73:343–351. [PubMed: 11199988]
21. Ceresa A, Radu A, Peper S, Bakker E, Pretsch E. Anal. Chem 2002;74:4027–4036. [PubMed: 12199570]
22. Mathison S, Bakker E. Anal. Chem 1998;70:303–309.
23. Qin Y, Peper S, Radu A, Ceresa A, Bakker E. Anal. Chem 2003;75:3038–3045. [PubMed: 12964748]
24. Long R, Bakker E. Anal. Chim. Acta 2004;511:91–95.

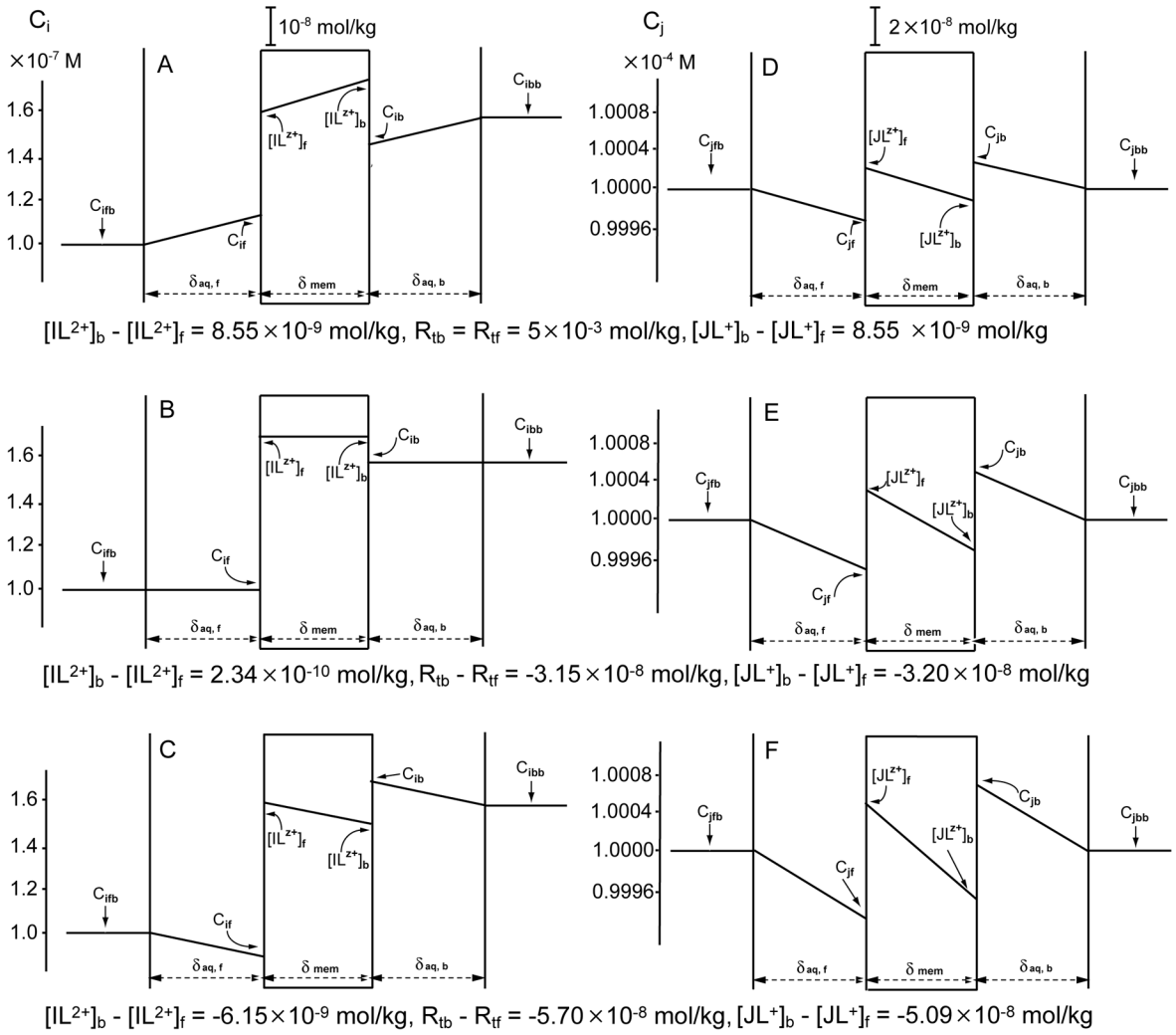

Fig. 1.

Schemes of primary and interference ion concentration profiles (A and D) before an external current is applied, (B and E) when the critical current is applied at which point the stir effect disappears, and (C and F) when more than the critical current is applied. The local ion concentrations are calculated for a model Pb^{2+}/H^{+} system (pH = 4.0). Parameters used: c_{ifb} = $10^{-7.0}$ M, c_{ibb} = $10^{-6.8}$ M, ρ_m = 2.2 × 10^{-5} dm s^{-1}, q_{stirred} = 1.57, $q_{\text{unstirred}}$ = 5.25, R_T = 0.005 mol/kg, and $K_{Pb,H}^{pot}=10^{-8.0}$. The calculated primary ion concentrations for the middle of the membrane correspond to $R_T/2$.

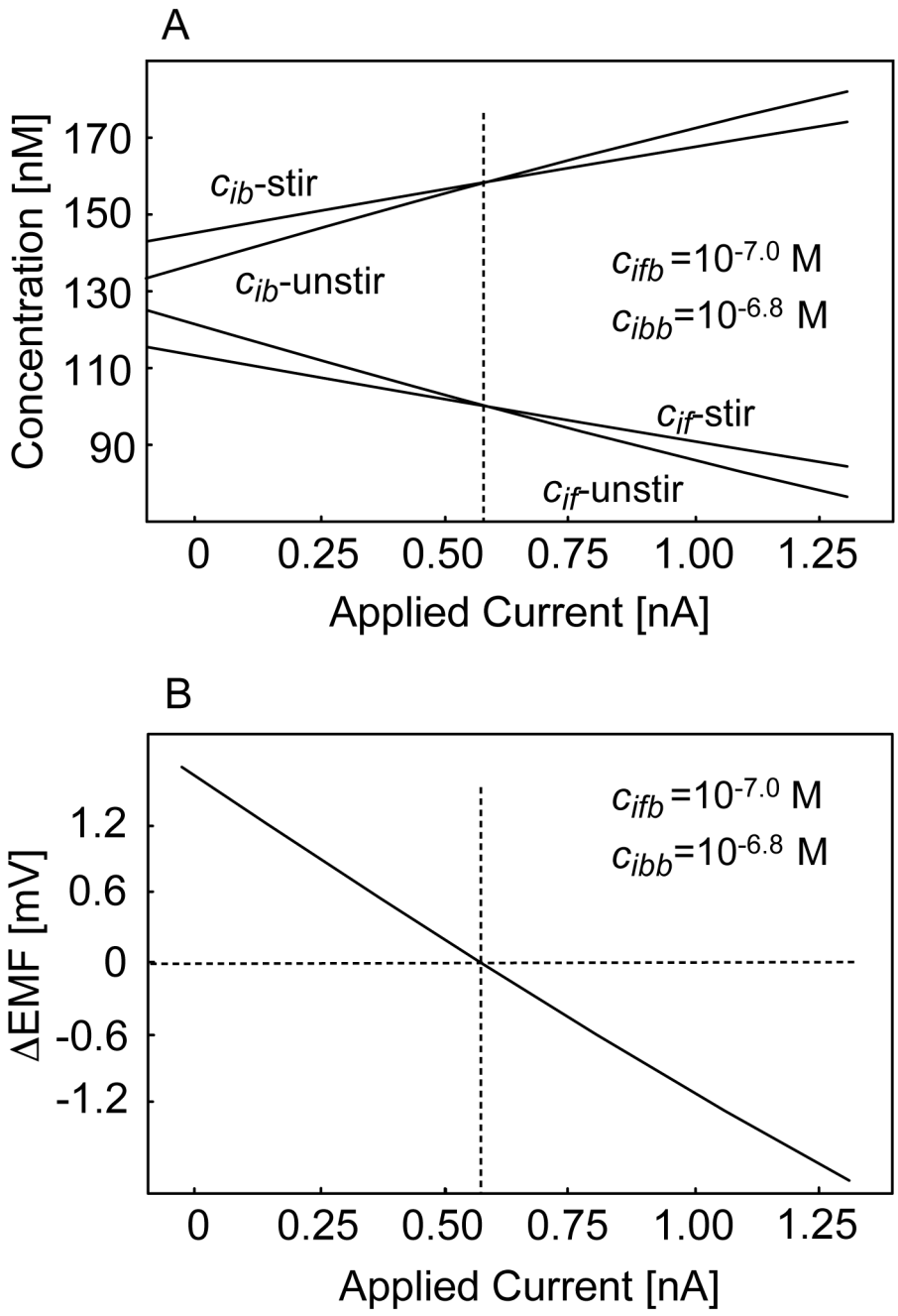

Fig. 2.

In the model Pb^{2+}/H^{+} system (pH = 4.0), (A) Theoretical changes of primary ion (lead) phase boundary concentrations when external current is applied; (B) Theoretical potential jump upon stop stirring when external current is applied. The parameters used in the calculation were: $c_{ifb} = 10^{-7.0}$ M, $c_{ibb} = 10^{-6.8}$ M, $\rho_m = 2.2 \times 10^{-5}$ dm s^{-1}, $q_{\text{stirred}} = 1.57$, $q_{\text{unstirred}} = 5.25$, R_T = 0.005 mol/kg, and $K^{pot}_{Pb,H}=10^{-8.0}$.

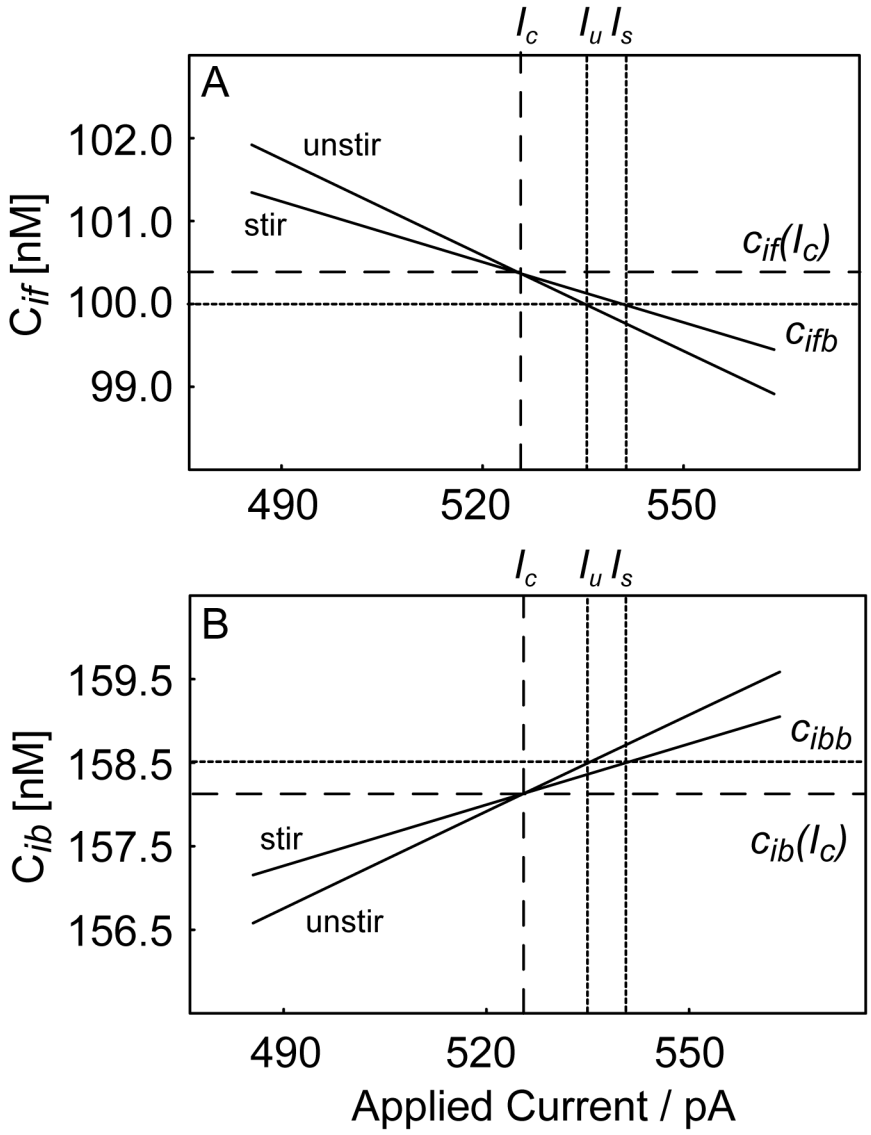

Fig. 3.

Theoretical changes of lead ion phase boundary concentrations (A) at the front side and (B) back side, when the current is very close to the critical current. I_c, calculated critical current where stir effect disappears; I_u, calculated current required to fully compensate the primary ion flux with unstirred solutions; I_s, calculated current fully compensate the primary ion flux with stirred solutions; $c_{if}(I_c)$ and $c_{ib}(I_c)$, phase boundary ion concentrations at the critical current. The parameters used in the calculation are the same as for Fig. 2.

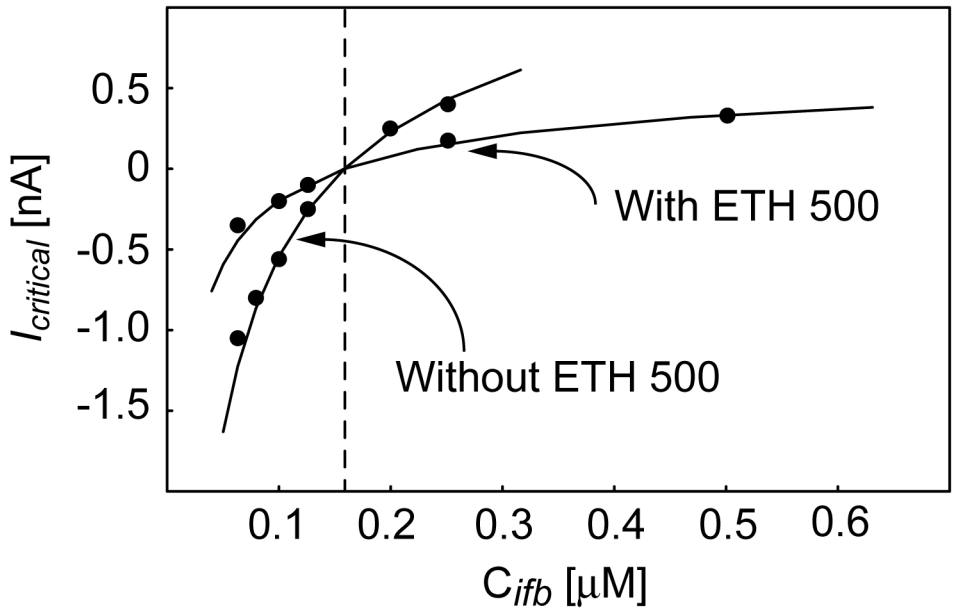

Fig. 4.

Theoretical and experimental critical currents required with different front side primary ion (lead) bulk concentrations (c_{ifb}) when the membrane cocktail is with and without ETH 500. The parameters used in the calculation were: $c_{ibb} = 10^{-6.8}$ M, $R_T = 0.005$ mol/kg, and $K^{pot}_{Pb,H} = 10^{-8.0}$. For the membrane with ETH 500, $q_{stirred} = 0.57$, $q_{unstirred} = 1.91$ and $\rho_m = 8 \times 10^{-6}$ dm s^{-1}; for the membrane without ETH 500, $q_{stirred} = 1.57$, $q_{unstirred} = 5.25$ and $\rho_m = 2.2 \times 10^{-5}$ dm s^{-1} (see also experimental part).

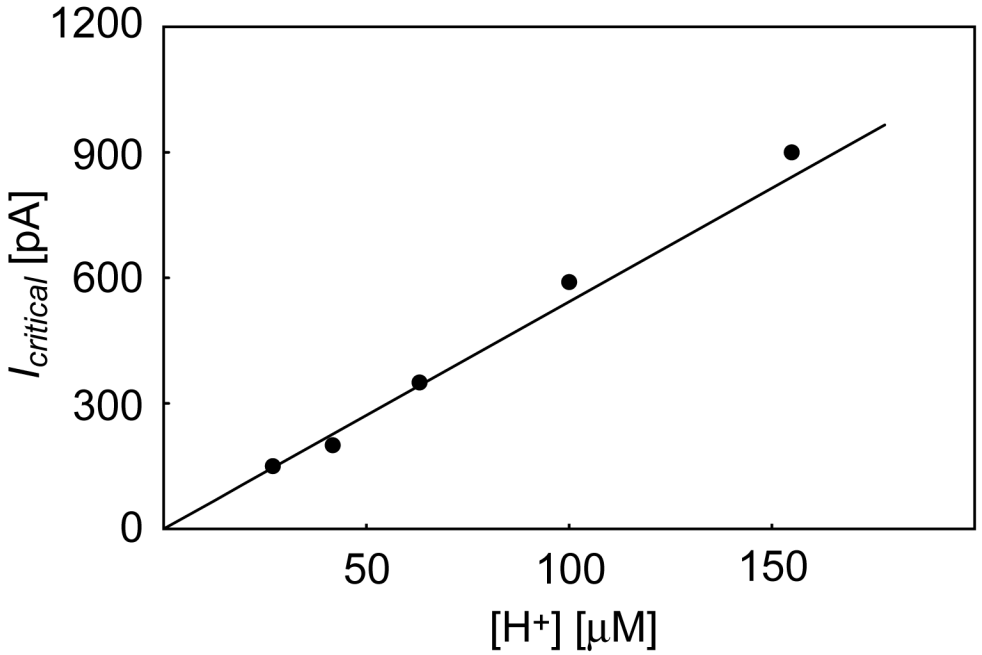

Fig. 5.

Theoretical (solid line) and experimental critical currents required for different pH values in the contacting solutions (concentration of dominant interference ions). The parameters used in the calculation are the same as for Fig. 2.

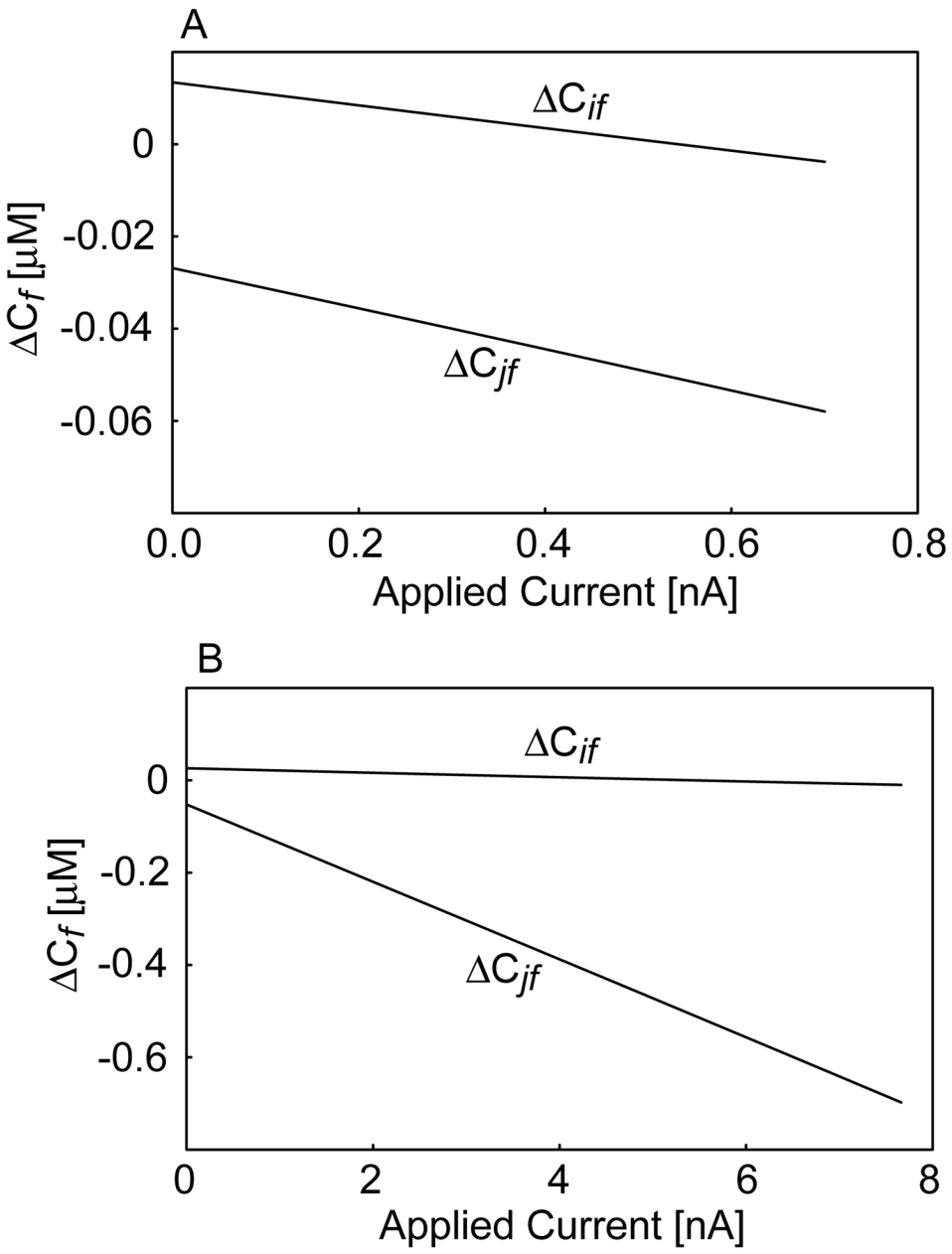

Fig. 6.

Theoretical primary ion (lead) front side concentration gradient with increased external current at (A) pH = 3 and (B) pH = 4. The parameters used in the calculation are the same as for Fig. 2.

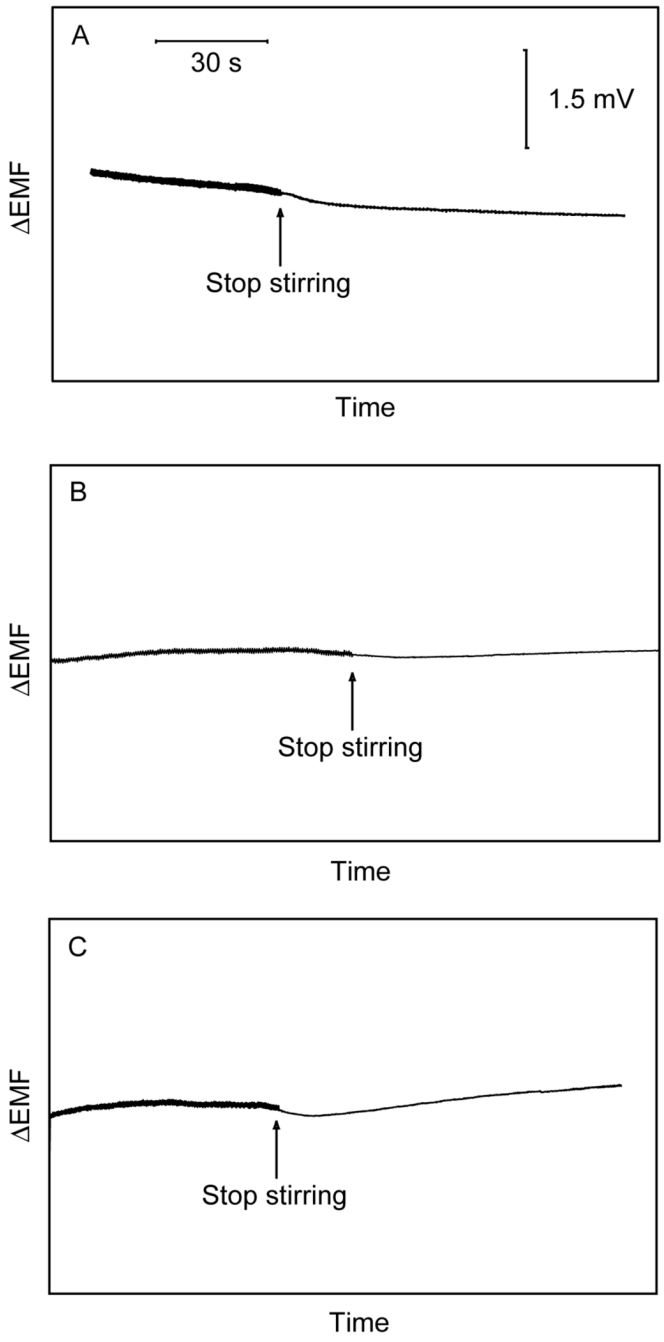

Fig. 7.

Time trace for the measurement of West Lafayette tap water. (A) Applied 100 pA current; (B) Applied 150 pA current; (C) Applied 200 pA current. The parameters used in the calculation were: $c_{ibb} = 4 \times 10^{-8}$ M, $q_{\text{stirred}} = 1.57$, $q_{\text{unstirred}} = 5.25$, $\rho_m = 2.2 \times 10^{-5}$ dm s^{-1}, $R_T = 0.005$ mol/kg, and $K_{Pb,H}^{pot} = 10^{-8.0}$.

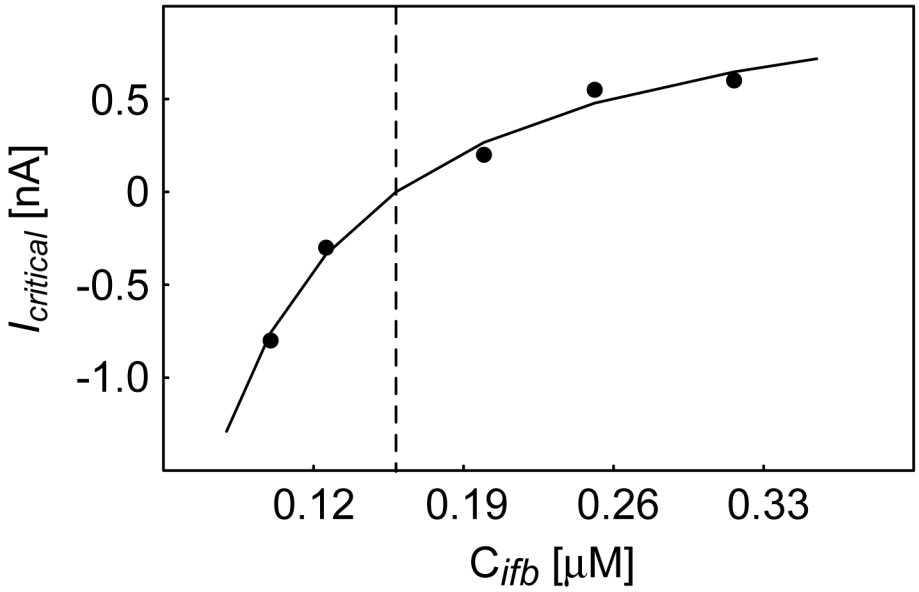

Fig. 8.

Theoretical and experimental critical current required with different calcium front side bulk concentrations when the backside concentration of calcium is fixed at $10^{-6.8}$ M. The parameters used in the calculation were: $q_{\text{stirred}} = 1.57$, $q_{\text{unstirred}} = 5.25$, $\rho_m = 3.4 \times 10^{-5}$ dm s^{-1}, $R_T = 0.005$ mol/kg, and $K^{pot}_{Ca,Mg} = 10^{-8.8}$.